ELSEVIER

Journal of Power Sources 53 (1995) 85–92

JOURNAL OF POWER SOURCES

Corrosion of lead and lead alloys: influence of the active mass and of the polarization conditions

J. Garche

Center for Solar Energy and Hydrogen Research Baden-Württemberg, Helmholtzstrasse 8, D-89081 Ulm, Germany

Received 7 September 1994; accepted 10 September 1994

Abstract

The influence of the active mass, as well as of discontinuous polarization (100 h at 6 mA cm^{-2}; 68 h at open circuit) on the corrosion rate of lead–antimony alloys has been measured with respect to samples without active mass and continuous polarization. During continuous polarizations two time regions have been found for the corrosion rate (v): during the first 75 h, the corrosion rate decreases according to $v \sim 1/t^{0.5}$ and then is constant during the remaining second period. An active-mass protection factor (PF_{AM}) describes the decrease of the corrosion rate in the presence of active mass; PF_{AM} is >2. Surprisingly, such a protection factor is also found in the presence of electronically isolating α-Al_2O_3. The influence of changes in potential, current density, pH and corrosion structure on the corrosion rate in the presence of active mass is discussed. The main influence comes from changes in the corrosion structure. A model is developed on the basis of diffusion of oxygen species through a dense corrosion layer. This corrosion layer grows to a critical thickness. After reaching this critical thickness, the layer divides into a inner dense and an outer porous zone as a result of relaxation in the internal mechanical stress that is created by the higher volume of the corrosion product. This model explains the time course of the corrosion rate, the action of the active mass and the influence of rest periods during polarization.

Keywords: Corrosion; Lead; Lead alloys; Active mass; Polarization conditions

1. Introduction

The influence of acid concentration, potential, current density or temperature on the corrosion rate of lead and lead alloys in sulfuric acid solution has been widely reported. By contrast, the influence of the active mass [1–10] and the polarization conditions [10] has received less attention. Experimental difficulties are the primary reason for this imbalance in investigations. The study reported here will try to give an explanation of the action of the active mass and polarization conditions on the corrosion rate, based on systematic experimental work and theoretical considerations.

2. Experimental

Fig. 1 shows the experimental apparatus used for the corrosion measurements. A cylindrical lead or lead–antimony rod was uniformly covered with active mass. Individual tubes of the type used in industrial tubular electrodes were employed, as described by Papazov et al. [10]. Typically, an unformed fresh paste was introduced into the tube by the use of nitrogen pressure (3.5 kP/cm^2). In order to vary the active mass density, dry commercial leady oxide (60 wt.% PbO) was vibrated into the tube at different intensities. A blend of α-Al_2O_3 and active material was introduced into the tube in the same way. The thickness of the active mass was varied at constant tube diameter (8 mm) by changing the diameter (normally 4 mm) of the lead/lead–antimony rod.

Electrode formation was carried out using the following standard procedure:

time:	72 h
temperature:	25 °C
current density:	10 mA per cm^2 of rod surface
sulfuric acid sp. gr.:	1.28 g cm^{-3}

The degree of corrosion was measured by evaluation of the weight loss of the rod after polarization and mechanically removing the active mass, and/or chemically dissolving the corrosion layer by boiling the samples in an alkaline (160 g l^{-1} NaOH) sugar solution (200 g l^{-1} saccharose).

SSDI 0378-7753(94)01978-5

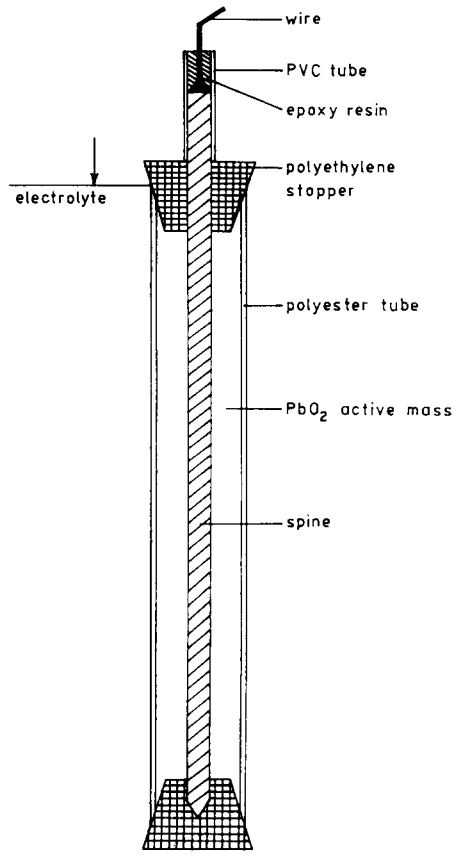

Fig. 1. Experimental apparatus for corrosion measurements on samples.

Continuous polarization was carried out in the galvanostatic mode, namely, 6 mA per cm^2 of rod surface. For discontinuous polarization, the following regime was used: (i) continuous galvanostatic polarization (6 mA per cm^2 rod surface) for 100 h; (ii) open-circuit rest for 68 h. All polarization experiments were performed in 4.93 M H_2SO_4 (1.28 sp. gr.) at 40 °C. The potential difference between the surface of the active mass and the surface of the rod was measured by using Luggin capillaries, as shown in Fig. 2.

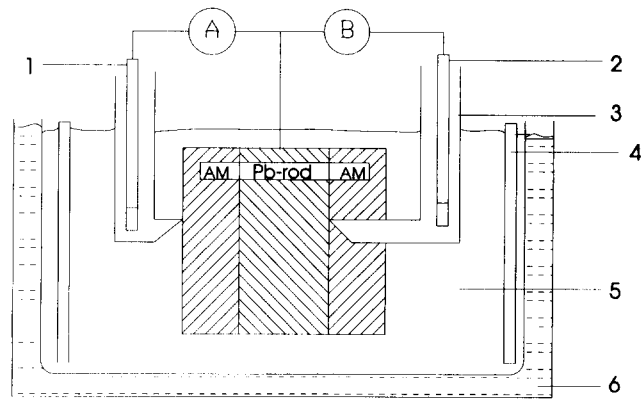

Fig. 2. Arrangement for measurement of the potential difference between the geometrical active-mass surface and the lead/lead alloy rod surface. 1,2 = Hg/Hg_2SO_4 reference electrodes, 3 = Luggin capillary, 4 = counter electrodes, 5 = electrolyte, 6 = water bath.

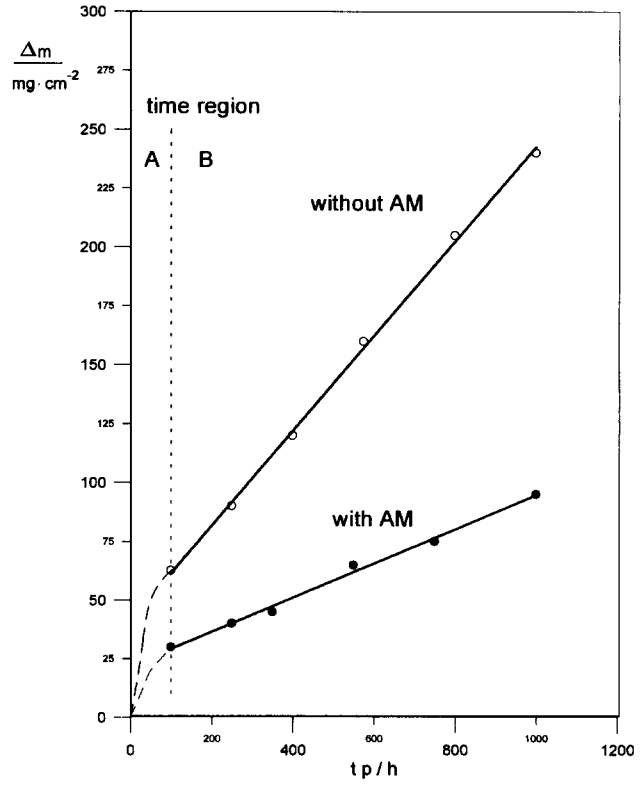

Fig. 3. Mass loss (Δm) vs. galvanostatic polarization time (t_p) for Pb–5.6wt.%Sb–0.15wt.%As alloy samples without and with active mass.

3. Influence of active mass

3.1. Mass loss

The weight loss (Δm) of a Pb–5.6wt.%–0.15wt.%As sample, both with and without active mass, as a function of the galvanostatic polarization time (t_p) is shown in Fig. 3.

For both samples, two time regions can be distinguished, namely: (A) $0 \leqslant t_p < 75$–100 h; (B) $t_p \geqslant 75$–100 h. It was difficult to fit an exact critical time value in each case, because the frequency of measurement was too low. Therefore, a time period of 75–100 h is given. In time region A, the corrosion rate v ($v = d\Delta m/dt_p$) decreases continuously. In time region B, the corrosion rate is independent of the polarization time. The value of this constant rate is used later to compare the corrosion behaviour of different samples.

In a separate experiment, the relationship between the weight loss and the polarization time for the same alloy without an active mass in the time region A was found to be:

$$\Delta m \sim t_p^{0.52} \quad (1)$$

This value is close to that found by Pavlov and Rogatchev [11], namely, $t_p^{0.47}$.

The presence of the active mass obviously leads to a decrease in the corrosion rate. In order to express this influence, an active-mass protection factor (PF_{AM}) is introduced as the ratio of the corrosion rate without active mass (v_{wo}) and with active mass (v_w), i.e.,

$$PF_{AM} = \frac{v_{wo}}{v_w} \quad (2)$$

Table 1 shows the protection factors for lead alloys with different antimony contents. As is well known, the corrosion rate increases with increasing antimony content in the alloy. It is remarkable, however, that the active mass protection factor decreases markedly from 7.5 for pure lead to 2.6 for the Pb–8 wt.% Sb alloy.

The influence of the thickness and the density of the active mass is shown in Tables 2 and 3, respectively. As expected, the corrosion rate decreases with increasing thickness or density of the active mass.

Table 1
Corrosion rate of samples with different antimony contents without active mass (v_{wo}) and with active mass (v_w), as well as the active mass protection factor (PF_{AM})

Antimony-content (wt.%)	v_{wo} (mg/cm²/h)	v_w (mg/cm²/h)	PF_{AM}
0	0.165	0.022	7.5
5	0.201	0.065	3.1
8	0.231	0.080	2.6

Table 2
Corrosion rate (v_w) and active-mass protection factor (PF_{AM}) for different thicknesses of active mass (alloy: Pb–5.6wt.%Sb–0.15wt.%As)

Active mass thickness (mm)	v_w (mg/cm²/h)	PF_{AM}
0 (without)	0.199	1
2	0.087	2.28
3	0.077	2.58

Table 3
Corrosion rate (v_w) and active-mass protection factor (PF_{AM}) for different densities of active mass (alloy: Pb–5.6wt.%Sb–0.15wt.%As)

Lead powder density (g cm⁻³)	v_w (mg/cm²/h)	PF_{AM}
0 (without)	0.199	1
1.93	0.087	2.28
2.34	0.082	2.42

3.2. Inert substances

One reason for the decrease in corrosion rate in the presence of active mass could be a decrease in the corrosion current density (I^{Pb}_{corr}) at the metal surface by introducing the high-area active mass (5 $m^2\ g^{-1}$) into the sample. In order to test this hypothesis, the active mass was blended with α-Al_2O_3 powder. The results of this experiment are shown in Table 4. Surprisingly, the electronically isolating Al_2O_3 also shows an influence on the corrosion rate of the lead–antimony rod.

3.3. Potential

The potential at the rod surface should also change in the presence of the active mass. Therefore, the potential of the sample was measured both at the geometrical surface of the active mass and at the surface of the rod, with the arrangement shown in Fig. 2. The results are given in Fig. 4. It can be seen that the potential curve reflects both the preparation period (formation at 25 °C and 10 mA cm^{-2}) and the subsequent corrosion period (polarization at 40 °C and 6 mA cm^{-2}).

The step in the potential curve is due to the different temperature and current conditions employed in the two periods. After about 10 days, a constant potential of 1345 mV is measured at the outside of the tube.

The potential difference between the geometrical surface of the active mass and the surface of the rod was 9 mV at the beginning of formation, 5 mV at the beginning of polarization (3 days), and 1 mV at the end of polarization (10 days).

The difference of the potential at the rod of samples with and without active mass amounted to 20 mV.

3.4. Sulfuric acid

A further reason for the change in the corrosion rate in the presence of active mass could be a decrease in the diffusion of protons, formed by anodic processes in the active mass. Therefore, the pH of the real corrosion medium is decreased. Table 5 illustrates the influence of different sulfuric acid concentrations on

Table 4
Dependence of corrosion rate (v_w) and active-mass protection factor (PF_{AM}) during continuous polarization on the mass content (special alloy: PbSb5)

Mass content		v_w (mg/cm²/h)	PF_{AM}
Active mass (vol.%)	α-Al_2O_3 (vol.%)		
0	0	0.223	1.00
0	100	0.157	1.42
50	50	0.152	1.47
100	0	0.138	1.62

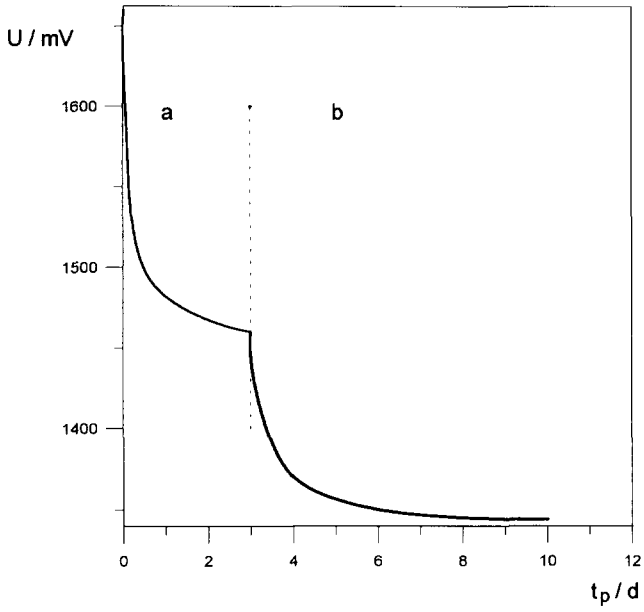

Fig. 4. Potential at geometric PbO_2 surface vs. anodic polarization time: Region a = formation (10 mA cm^{-2}, 25 °C); region b = polarization (6 mA cm^{-2}, 40 °C). For measurement arrangement see Fig. 2.

Table 5
Mass loss (Δm) after 10 days polarization as a function of sulfuric acid density (alloy: Pb–5.6wt.%–0.15wt.%As)

Sulfuric acid density (g cm^{-3})	Δm (mg cm^{-2})
1.28	82.0
1.34	83.6
1.40	88.4

the mass loss. As expected, the corrosion rate increased slightly with increasing sulfuric-acid density.

4. Influence of polarization conditions

4.1. Samples without active mass

At first sight, the curves of the mass loss for discontinuous polarization (6 mA cm^{-2} for 100 h; open circuit for 68 h) show the same general shape (i.e. two time regions) as the curves for the continuous polarization tests. This should be attributed, however, to the frequency of the mass-loss determination. In general, the measurement was undertaken only every 168 h (one period). Thus, a separation of the contributions due to the polarization and the open-circuit periods was impossible. This fact must be taken into consideration when comparing the corrosion rate values for continuous (v^{con}) and discontinuous polarization (v^{dis}), as shown in Table 6.

Table 6
Comparison of corrosion rate of different samples, without active mass, during discontinuous polarization (v^{dis}) and continuous polarization (v^{con})

Antimony content (wt.%)	v^{dis} (mg/cm^2/h)	v^{con} (mg/cm^2/h)	v^{dis}/v^{con}
0	0.117	0.165	0.71
5	0.145	0.201	0.72
8	0.160	0.231	0.69

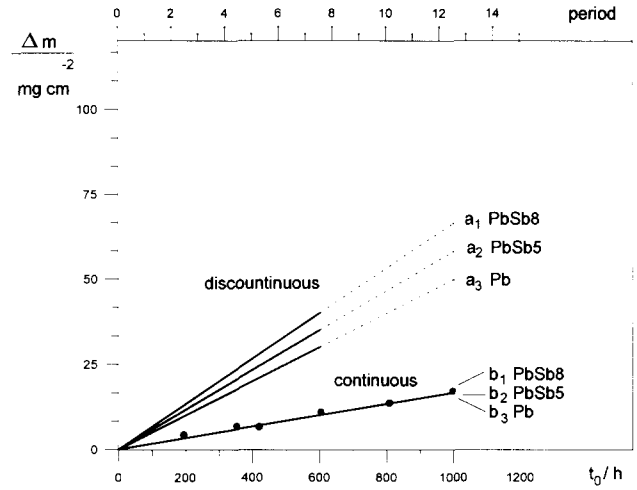

Fig. 5. Mass loss during the open-circuit rest period (t_0). Plots a = calculated by Eq. (5), discontinuous polarization; plots b = measured by continuous open-circuit experiment.

Note, the total time (t_t) is the sum of the polarization time (t_p) and the rest time (t_r), i.e.,

$$t_t = t_p + t_0 \quad (3)$$

No major changes in the corrosion rate relation (v^{dis}/v^{con}) were found with change in the antimony content of the alloys.

In accordance with Eq. (3), the total mass loss (Δm_t) consists of the polarization part (Δm_p) and the rest period part (Δm_o), i.e.,

$$\Delta m_t = \Delta m_p + \Delta m_o \quad (4)$$

Thus, the mass loss due to corrosion during the rest period (Δm_o) can be calculated as:

$$\Delta m_o = \Delta m_t - \Delta m_p \quad (5)$$

The mass loss under continuous polarization (Δm_p) was taken from the data listed in Table 1. The open-circuit mass loss in the discontinuous polarization calculated by Eq. (5) is compared in Fig. 5 with the open-circuit mass loss measured during a continuous experiment. A large difference is found between the two sets of values.

To study in more detail the corrosion rate under discontinuous testing, the mass loss was determined

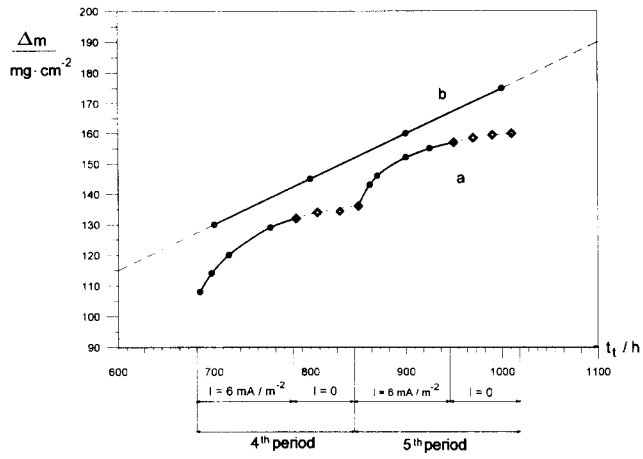

Fig. 6. Mass loss during discontinuous (4th and 5th period) and continuous polarization (t_p = 400–600 h).

every 20 h during the course of the fourth and fifth discontinuous period, see Fig. 6. It can be seen that the corrosion rate during discontinuous testing is not constant. The rate is relatively high at the start of the polarization phase of every period and then decreases.

4.2. Samples with active mass

For samples with active mass, the mass loss during discontinuous polarization (6 mA cm^{-2} for 100 h; open-circuit for 68 h) is shown in Table 7 as a function of the total test time (t_t), and is also compared with the continuous polarization values (taken from Table 1).

It is obvious that the corrosion under continuous polarization is higher than under discontinuous polarization, except in the case of the pure lead. Surprisingly, the active-mass protection factor for discontinuous polarization increases slightly with increasing antimony content of the alloy.

A real separation of the mass loss during the polarization phase (Δm_p) and the rest period (Δm_o) was determined for one alloy by measuring the mass loss after every polarization and rest period (see Table 8).

The ratio of the corrosion rate during the polarization part to that during the rest part is about 3:1. Moreover, the corrosion in the polarization part of the discontinuous test is higher than that in the continuous mode.

5. Discussion

From a theoretical point of view, the following points should be taken into consideration to explain the action of both the active mass and the open-circuit rest periods on the corrosion behaviour.

5.1. Change of corrosion potential

The corrosion potential at the rod during the galvanostatic polarization is decreased by 20 mV if active mass is introduced into the sample. This should have a slight influence on the protection factor.

5.2. Change of current density

The total current density (6 mA cm^{-2}) is divided into partial current densities in accordance with the following equations:

without active mass: $I = I^{Pb}{}_{corr} + I^{Pb}{}_{Ox}$ (6)

with active mass: $I = I^{Pb}{}_{corr} + I^{Pb}{}_{Ox} + I^{AM}{}_{Ox}$ (7)

where: $I^{Pb}{}_{corr}$ is the corrosion current on the rod; $I^{Pb}{}_{Ox}$ is the oxygen evolution current on the rod; $I^{AM}{}_{Ox}$ is the oxygen evolution current on the active mass.

An addition of high-area (5 $m^2\ g^{-1}$) active mass into the sample leads to an increase of the real sample surface by a factor of 10^5. Therefore, the corrosion current density ($I^{Pb}{}_{corr}$) should decrease dramatically.

As the above experimental results with electronically isolating α-Al_2O_3 have shown, addition of electronically isolating α-Al_2O_3 decreases the corrosion rate by the same order as the active masses. Therefore, the current density change is not the main reason for the active mass action.

5.3. Change of corrosion pH

A decrease in pH during the anodic polarization should be observed, due to the proton formation both in the active mass and at the surface of the rod, i.e.,

$$Pb + 2H_2O + 4e^- \longrightarrow PbO_2 + 4H^+ \quad (8)$$

$$H_2O + 2e^- \longrightarrow \tfrac{1}{2}O_2 + 2H^+ + 2e^- \quad (9)$$

The diffusion of these protons can be hindered by the active mass [12]. This leads to a decrease in the pH at the rod. This could be a source of a change in the

Table 7
Comparison of corrosion rate of samples with active mass during discontinuous polarization (v^{dis}) and continuous polarization (v^{con}). Protection factors for discontinuous (PF^{dis}) and continuous polarization (PF^{con}) are also given

Antimony content (wt.%)	v^{dis} (mg/cm²/h)	v^{con} (mg/cm²/h)	v^{dis}/v^{con}	PF^{dis}	PF^{con}
0	0.055	0.022	2.5	2.12	7.5
5	0.061	0.065	0.9	2.37	3.1
8	0.065	0.080	0.8	2.46	2.6

Table 8
Comparison of the contributions of the different test phases on the corrosion rate (v) of a Pb–5.6wt%Sb–0.15wt.%As alloy with active mass

Polarization mode	Corrosion rate, v (mg/cm²/h)		
	Test test, t_t $d\Delta m/dt_t$	Polarization time, t_p $d\Delta m/dt_p$	Rest time, t_0 $d\Delta m/dt_0$
Discontinuous	0.105	0.146	0.046
Continuous	0.138	0.138	

corrosion rate. Experimental results show, however, that an increase in sulfuric acid concentration from 1.28 to 1.40 g cm^{-3} increases the corrosion rate by about 8%. Therefore, the pH phenomenon could not be the reason for the decrease in the corrosion rate in the presence of active mass.

5.4. Change of corrosion-layer structure

Changes in corrosion-layer structure should be the main cause of the active-mass action and the polarization regime. This will be explained on the basis of the following model, which is based partially on considerations of Pavlov and Rogatchev [11] and Astachov et al. [13].

5.4.1. Time region A

The corrosion takes place via an ionization of lead at the lead/corrosion-layer interface together with a transport of oxygen species (ions or vacancies) [11] (Fig. 7) through a dense layer (see Fig. 8(b)). The rate-determining step for corrosion is the relatively low transport of oxygen species by diffusion and migration through the dense corrosion layer, i.e.,

$$j_O = -\frac{Dc}{RT}\left(\frac{d\mu}{dl_d} + zF\frac{d\theta}{dl_d}\right) \quad (10)$$

where: j_O is the flux oxygen species; D is the diffusion coefficient; c is the concentration of the oxygen species; μ is the chemical potential; θ is the Galvani potential; l_d is the thickness of the dense part of the corrosion layer.

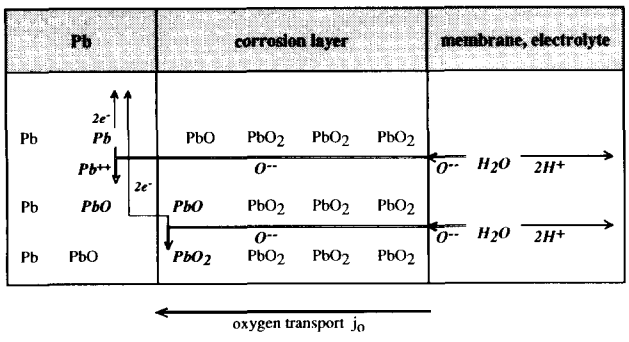

Fig. 7. Schematic of the mechanism of lead corrosion.

5.4.2. Time region B

At the beginning of polarization, the corrosion layer grows as a dense layer. After a longer polarization time, part of the corrosion layer becomes porous. Due to the higher molar volume of the corrosion product (PbO_2) compared with lead ($V_{PbO_2}/V_{Pb} = 1.35$), an internal mechanical stress is formed in the corrosion layer. At a critical thickness of the dense layer (Fig. 8(c)), the stress is offset by the layer dividing into an inner, dense and a outer, porous sub-layer (Fig. 8(d)).

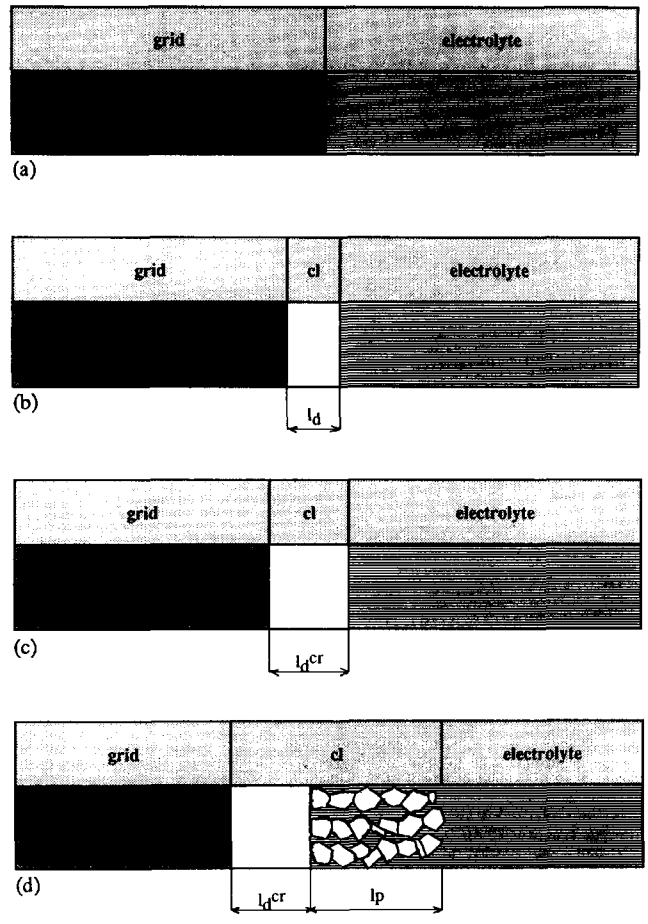

Fig. 8. Schematic of the growth of the corrosion layer in different phases of polarization: (a) before start of polarization; (b) start of polarization; (c) intermediate time; (d) after long polarization. i_d = thickness of dense part of corrosion layer, i_d^{cr} = critical thickness of dense part of corrosion layer, i_p = thickness of porous part of corrosion layer.

The relaxation of this stress has been proved by ultrasonic measurements [14].

During polarization, the mechanical stress in the dense layer after the relaxation is approximately constant; therefore, the critical thickness will also be constant. Thus, a dense layer of constant thickness is formed during the polarization and shifts in the direction of lead by increasing of the porous zone (Fig. 8(d)). In practice, cracks are formed by relaxation of the mechanical stress and these can extend through to the lead surface. They will, however, be filled immediately by corrosion products via a solution/precipitation reaction.

5.4.3. Rest period (time region C)

Early in the rest period, the relaxation of the internal mechanical stress takes place further [14]. This leads to a total porous corrosion layer, e.g., the dense PbO_2 layer also becomes a porous layer. Further, the corrosion layer PbO_2 reacts with both the electrolyte [11] and the lead [12,15]:

$$PbO_2 + H_2SO_4 \longrightarrow PbSO_4 + \tfrac{1}{2}O_2 + H_2O \quad (11)$$

$$PbO_2 + Pb + 2H_2SO_4 \longrightarrow 2PbSO_4 + 2H_2O \quad (12)$$

Therefore, the PbO_2 is changed partially into $PbSO_4$ which also increases the internal mechanical stress. The corrosion reaction [12] is as fast as the corrosion layer is porous [15].

The experimental facts given above will be discussed on the basis of the model shown in Sections 5.4.1.–5.4.3.

5.5. Continuous polarization

5.5.1. Corrosion in time region A

At the beginning of polarization, i.e., in time region A, the experimental conditions are constant. Therefore, all values in Eq. (10) are also constant, except for the thickness of the dense part of the corrosion layer (l_d) which continues to increase. Eq. (10) is reduced to:

$$j_O \approx \frac{\text{const.}}{l_d} \quad (13)$$

By setting:

$$\frac{dl_d}{dt} \sim j_O \quad (14)$$

one obtains, with Eq. (13):

$$\frac{dl_d}{dt} = \frac{\text{const.}}{l_d} \quad (15)$$

Integration of Eq. (15) yields:

$$l_d^2 = \text{const. } t \quad (16)$$

or

$$l_d = \text{const. } t^{0.5} \quad (17)$$

With:

$$l_d \sim \Delta m \quad (18)$$

then:

$$\Delta m = \text{const. } t^{0.5} \quad (19)$$

As discussed above, approximately the same relation (viz., $\Delta m \sim t^{0.52}$) was found, experimentally, in the time region A for the Pb–5.6 wt.%Sb–0.15 wt.%As alloy.

5.5.2. Corrosion in time region B

After the dense corrosion layer reaches its critical thickness (l_d^{cr}) all values, including l_d^{cr}, are constant in Eq. (10). Therefore, this equation can be simplified to:

$$j_O \approx \text{const.} \quad (20)$$

Analogous to Eq. (15):

$$\frac{dl_d}{dt} = \text{const.} \quad (21)$$

and analogous to Eqs. (16)–(18), the mass loss is given by:

$$\Delta m = \text{const. } t \quad (22)$$

This relation was confirmed experimentally in all cases.

5.6. Discontinuous polarization

The discontinuous polarization sequence is as follows.

First period:

a – 75 h: corrosion in accordance with time region A ($\Delta m = \text{const. } t^{0.5}$)
25 h: corrosion in accordance with time region B ($\Delta m = \text{const. } t$)

b – dense layer becomes porous according to Eqs. (11) and (12) (time region C)

Second period:

c – this period starts with a porous layer, i.e., a dense layer will build up again
Therefore, in a first approximation:
75 h: corrosion in time region A ($\Delta m = \text{const. } t^{0.5}$)
25 h: corrosion in time region B ($\Delta m = \text{const. } t$)

d – the dense layer becomes porous again according to Eqs. (11) and (12) (time region C)

e,f – repeat of sequence

This is shown schematically in Fig. 9 for the continuous polarization period.

5.7. Action of the active mass

As shown above, the active mass leads to a decrease in the corrosion rate. The reason for this is the increase of the critical thickness of the dense corrosion layer as a consequence of a partial compensation for the internal mechanical stress that is created by external

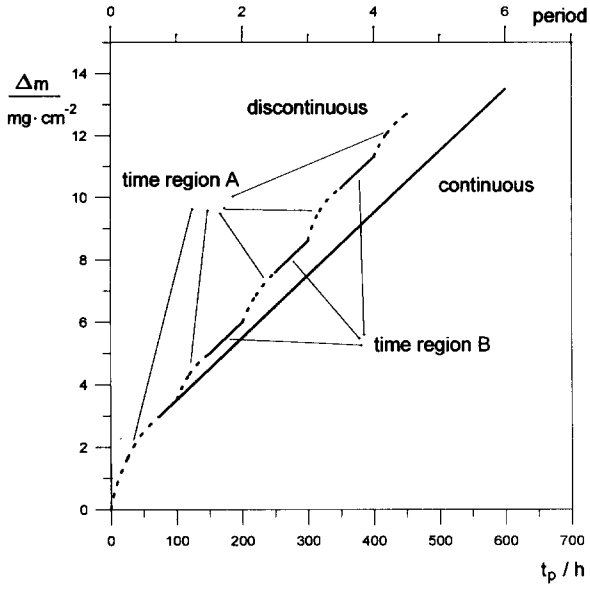

Fig. 9. Schematic of mass loss (Δm) vs. polarization time (t_p): a = continuous polarization; b = discontinuous polarization.

forces. Therefore, the value of l_d^{cr} in Eq. (10) is increasing and the corrosion rate decreases. This partial compensation will be greater with increase in the density (Table 3) or the thickness (Table 2) of the active mass.

The decrease in the corrosion rate caused by α-Al_2O_3 can also be explained by partial compensation of the mechanical stress.

The increase in the critical thickness of the dense corrosion layer and, therefore, the decrease of the corrosion rate should be the greater, the higher the internal stress. The strongest stress is expected at pure lead and this should be decreased with increasing antimony content of the alloy. This is because the molar volume of the corrosion product of lead–antimony alloys is lower than that of pure lead [16].

During continuous polarization the active-mass protection factor for pure lead is therefore the highest ($PF_{AM} = 7.5$) and is reduced with increasing Sb content of the alloy (see Tables 1 and 7). At discontinuous polarization, however, where the critical thickness of the dense corrosion layer will be built up only at the end of every polarization phase (100 h), the active-mass protection factor is in a first approximation independent of the antimony content of the Pb alloy (see Table 7).

Acknowledgements

The author thanks his former colleagues and students of the Dresden University of Technology for performing most of the experimental work, especially Angelika Dietz and Detlef Frenzel. Thanks are also due to Klaus Wiesener, Hartmut Dietz and Harry Döring for their helpful discussions. The assistance of D. Pavlov and T. Rogatchev (Central Laboratory of Electrochemical Power Sources, Bulgaria) for preparing some of the samples with active mass is also gratefully acknowledged.

References

[1] J.J. Lander, *J. Electrochem. Soc., 98* (1951) 213, 220.
[2] S. Feliu, L. Galan and J.A. Gonzales, *Werkst. Korros., 23* (1973) 554.
[3] Anon., *Lead Res. Dig., 31* (1973) 16.
[4] S. Feliu, E. Otero and J.A. Gonzales, *J. Power Sources, 3* (1978) 145.
[5] A.C. Simon and S.M. Caulder, *J. Electrochem. Soc., 121* (1974) 531.
[6] A.G. Cannone, D.O. Feder and R.V. Biagetti, *Bell System Tech. J., 49* (1970) 1335.
[7] G.W. Mao, J.G. Larson and P. Rao, *J. Electrochem. Soc., 120* (1973) 11.
[8] G. Kaden and B. Beyer, *Korrosion, 5* (1974) 18.
[9] T. Rogatchev, G. Papazov and D. Pavlov, *Prog. Batteries Solar Cells, 2* (1979) 145.
[10] G. Papazov, T. Rogatchev, D. Pavlov, J. Garche and K. Wiesener, *J. Power Sources, 6* (1981) 15.
[11] D. Pavlov and T. Rogatchev, *Electrochim. Acta, 23* (1978) 1237.
[12] J. Garche, K. Wiesener and H. Dietz, *Z. Phys. Chem., 263* (1982) 305.
[13] I.I. Astachov, I.G. Kiselova and B.N. Kabanov, *Dokl. Akad. Nauk SSSR, 154* (1964) 1414.
[14] H. Niepraschk, H. Döring and J. Garche, *UNESCO Workshop Theory and Practice of the Lead/Acid System*, Gaußig, Germany, 1991, lecture.
[15] J. Garche, *J. Power Sources, 31* (1990) 47.
[16] A.C. Simon, *J. Electrochem. Soc., 114* (1967) 1.